

Prashant Srivastav, Aadesh K. Prajapati, Pramod K. Yadawa*

Theoretical Investigation on Thermal, Mechanical and Ultrasonic Properties of Zirconium Metal with Pressure

*Department of Physics, Prof. Rajendra Singh (Rajju Bhaiya) Institute of Physical Sciences for Study and Research,
V. B. S. Purvanchal University, Jaunpur, India, *pk Yadawa@gmail.com*

Zirconium (Zr), a metal with an hcp structure, has been investigated for the transmission of acoustic wave in the 0 to 25 GPa operating pressure. For this, the Lennard-Jones interaction potential approach has been used to estimate the higher order elastic coefficients (SOECs and TOECs). This model is used to calculate the 2nd and 3rd order elastic parameters for zirconium metal. With the help of SOECs, other elastic moduli such as bulk modulus (B), Young's modulus (Y) and shear modulus (G) have been calculated for Zr metal using Voigt-Reuss-Hill (VRH) approximations. Later, applying SOECs as well as zirconium density under the same pressure range, three orientation dependent acoustic velocities, comprising Debye average velocities, have been studied. Basic thermal characteristics such as specific heat at constant volume, thermal conductivity associated with lattice, thermal energy density, thermal relaxation time as well as acoustic coupling coefficients of zirconium metal have been also calculated at same pressure range. The computation is also satisfactory in estimating the ultrasonic attenuation coefficients, arises due to the interaction of phonons, hardness as well as melting temperature under various pressures in this research work.

Keywords: ultrasonic properties, elastic constants, thermo-physical characteristics, thermal conductivity.

Received 17 November 2022; Accepted 21 September 2023.

Introduction

Due to its great corrosion protection as well as narrow neutron absorption cross - sectional area, zirconium is an interesting 4d transition metal that is employed extensively in the nuclear, chemical, & medicinal industries. Zirconium recrystallize in the "phase" at ambient temperatures, which is a hexagonal close-packed shape. It changes to a bcc structure beyond 1135 K with atmospheric pressure, known as that of the phase. Whenever pressure rises, α phase zirconium (P63/mmc) changes into a different hexagonal structure known as the ω -phase (P6/mmm), which isn't tightly packed and contains three atoms in each cell [1, 2]. When pressure has been released, the zirconium can also be retrieved as a thermodynamically stable phase under ambient circumstances [3, 4]. Zirconium-based alloys (Zr-Fe, Zr-Co, Zr-Ni, Zr-Cu) have also shown the ω -phase (P6/mmm) structure, which is an intriguing phenomena

that has drawn a lot of theoretical as well as experimental attention [5, 6]. Zirconium undergoes a martensitic kind of phase transition. Its atomic packing within this phase is 2.4% higher efficient than that of the phase as a result of crystal reconstruction, which might theoretically result in better mechanical characteristics [7]. In fact, Nanoindentation studies reveal that the high pressure-recovered ω -phase Zr is 80% harder than the α -Zr [8]. Further diffraction pattern investigation of microscopic strain by Zhao & Zhang also revealed transformation of the ω -phase Zr [9]. These results imply that an efficient method for material hardening is Stress-induced phase transitions resulting to qualitative data under ambient conditions. However, it has yet to be determined for ω -Zr what the constitutive law and associated deformation process are in its stability field. Because of their low weight, static strength, significant stiffness, as well as the fact that they do not disintegrate quickly as the temperature increases & exhibit resistance to oxidation, such materials have innovative uses in the aircraft sector

[10]. Adjusting the crystalline phases in such elements can significantly enhance their mechanical characteristics. In these kinds of materials, pressure is a crucial factor in the phase changes that result. Recent research by Cerreta et al. [11] using a shock experiment determined the pressure of the phase transformation for the highly pure material to be 7.1 GPa. Theoretically, several studies use electronic structures have been conducted on the phase transformations of Zr [12]. At extreme pressures, they have typically discovered a transition form. However, they found by experimentally that it has hexagonal close - packed phase except at least phase.

However, a solid's physical properties are crucial because they correlate to a number of essential solid-state characteristics, including interatomic potentials, equations of state, as well as phonon spectra. Additionally, the specific heat at constant volume, anisotropy constant, thermal attenuation, Debye temperature, thermal relaxation time, Poisson's ratio, Young's modulus (Y), Bulk modulus (B), Paugh ratio (B/G), shear modulus (G), melting temperature as well as hardness are all thermodynamically related to elastic characteristics.

I. Theoretical Calculation Method

There are numerous tools for analyzing hexagonal compounds' high-order (SOECs, TOECs) elastic properties. According to our current efforts, higher order elastic constants are being evaluated utilizing interaction-potential techniques.

By using potential model method of evaluation shows that, the higher order coefficients in hexagonally arranged materials are influenced by the crystallite size. The following mathematical formulas can be consumed to determine the second order elastic coefficients. [13]

$$C_{IJ} = \frac{\partial^2 U}{\partial e_i \partial e_j}; \quad I \text{ or } J=1, \dots, 6 \quad (1)$$

$$C_{IJK} = \frac{\partial^3 U}{\partial e_i \partial e_j \partial e_k}; \quad I \text{ or } J \text{ or } K=1, \dots, 6 \quad (2)$$

Where $e_i = e_{ij}$ (i or $j = x, y, z, I=1 \dots 6$) stands for a constituent of the tensor of strain as well as U shows elastic energy band. For hcp structural materials, Eqn. 1 as well as Eqn. 2, yields six 2nd order and ten 3rd order elastic constants, respectively (SOEC and TOEC) [14, 15].

For acoustic propagation via a z-axis in hcp crystal, the acoustic velocities (V_s and V_L) are provided by equations. [15]

$$V_L = \sqrt{\frac{C_{33}}{\rho}}, \quad (3)$$

$$V_S = \sqrt{\frac{C_{44}}{\rho}}. \quad (4)$$

The density of hcp materials can be evaluated consuming the mathematical formulae given below. [16]

$$\rho = 2Mn/3\sqrt{3}a^2cN_A \quad (5)$$

The letters n , M , as well as N_A , respectively, stand for the the number of atoms in unit cell, molecular mass, as well as Avogadro number.

Within low-temperature acoustics, the Debye average velocity (V_D) is an important number since acoustic velocities are connected to elastic coefficients. The Debye average velocity (V_D) is defined as [15].

$$V_D = \left[\frac{1}{3} \left(\frac{1}{V_L^3} + \frac{1}{V_{S1}^3} + \frac{1}{V_{S2}^3} \right) \right]^{-1/3} \quad (6)$$

Through Debye average velocity, Elastic coefficients are correlated to Debye temperature (T_D) in an unintended way. [17]

$$T_D = \hbar V_D (6\pi^2 n_a)^{1/3} / k_B \quad (7)$$

Where k_B , n_a are Constant of Boltzmann and atomic proportions constant respectively. The transmission of ultrasonic waves disrupts thermodynamic phonons' energy dispersion. The length of time required for thermal acoustic waves to re-establish just after acoustic wave has passed through a material is known as that of the thermal relaxation time (τ). It is directly connected to specific heat (C_v), thermal conductivity, Debye average velocity. [14, 18]

$$\tau = \tau_s = \tau_L / 2 = \frac{3k}{C_V V_D^2} \quad (8)$$

The modulus of shear and the bulk elastic coefficient were estimated by using Voigt and Reuss approaches [19, 20]. The Voigt and Reuss approaches used unvarying stress as well as strain calculations, respectively. Moreover, using Hill's approaches, the expectation values of mutually procedure are consumed to compute the numerical values that result of B as well as G [21]. Young's modulus (Y) as well as Poisson's ratio are computed by consuming the shear as well as bulk modulus numerical values [22, 23]. G , B , and Y are evaluated using the following expressions:

$$\left. \begin{aligned} M &= C_{11} + C_{12} + 2C_{33} - 4C_{13}, C^2 = (C_{11} + C_{12})C_{33} - 4C_{13} + C^2_{13}; \\ B_R &= \frac{C^2}{M}; B_V = \frac{2(C_{11} + C_{12}) + 4C_{13} + C_{33}}{9}; \\ G_V &= \frac{M + 12(C_{44} + C_{66})}{30}; G_R = \frac{5C^2 C_{44} C_{66}}{2[3B_V C_{44} C_{66} + C^2(C_{44} + C_{66})]}; \\ Y &= \frac{9GB}{G + 3B}; \quad B = \frac{B_V + B_R}{2}; \quad G = \frac{G_V + G_R}{2}; \quad \sigma = \frac{3B - 2G}{2(3B + G)} \end{aligned} \right\} \quad (9)$$

The following mathematical formula can be used to determine a metal's thermal conductivity. [24]

$$k = AMT_D^3 \delta^3 / \gamma^2 T n^{2/3} \quad (10)$$

Where A is the constant, γ is Grüneisen quantity, as well as T stands for temperature. The value, 'A' is calculated by the Grüneisen quantity as well as is expressed as follows.

$$A = 2.43 \times 10^{-8} / (1 - \frac{0.514}{\gamma} + \frac{0.228}{\gamma^2}) \quad (11)$$

The elastic constants C_{11} and C_{33} are correlated to the Temperatures that melt (T_m) of hexagonally structured materials [25]. The melting point (T_m) is calculated in the following way:

$$T_m = 354 + 4.5(2C_{11} + C_{33})/3 \quad (12)$$

Where C_{11} and C_{33} are in GPa and T_m is in K.

At low temperatures, the average distance travelled by electrons is analogous to the average route of acoustical phonons. As a result, acoustic phonons and free electrons have a high possibility of interacting [15]. For longitudinal (V_L) as well as shear waves (V_s), the mathematical expressions for evaluating ultrasonic attenuation is given as follows:

$$\alpha_{long} = \frac{2\pi^2 f^2}{\rho V_L^3} \left(\frac{4}{3} \eta_e + \chi \right) \quad (13)$$

$$\alpha_{shear} = \frac{2\pi^2 f^2}{\rho V_s^3} \eta_e \quad (14)$$

Where 'f' seems to be the acoustic wave's frequency, ' ρ ' is the density of hcp metal, ' η_e ' is the viscosity due to the electron as well as ' χ ' is the viscosity due to compression. Thermo-elastic loss and Akhiezer's type loss are mutually important for acoustic wave attenuation at greater pressure. The mathematical equation which is shown below describes the attenuation due to the Akhiezer loss obtained by Rai et. al. [27].

$$(\alpha/f^2)_{Akh} = \frac{4\pi^2 \tau E_0 (D/3)}{2\rho V^3} \quad (15)$$

Thermodynamically generated energy density is denoted by E_0 , where as the ultrasound wave's frequency is denoted by f.

The mathematical expression which is given below, considers the thermo-elastic loss $(\alpha/f^2)_{Th}$:

$$(\alpha/f^2)_{Th} = 4\pi^2 \langle \gamma_i^j \rangle^2 \frac{kT}{2\rho V_L^5} \quad (16)$$

The following equation gives the total ultrasonic attenuation as:

$$(\alpha/f^2)_{Total} = (\alpha/f^2)_{Th} + (\alpha/f^2)_L + (\alpha/f^2)_S \quad (17)$$

Where $(\alpha/f^2)_{Th}$ is the thermoelastic loss, $(\alpha/f^2)_L$ and $(\alpha/f^2)_S$ are the acoustic attenuation constants for the longitudinal acoustic wave as well as shear acoustic wave consistently.

II. Results and Discussion

2.1. Second Order Elastic Constants (SOECs), Third Order Elastic Constants (TOECs) and Related Parameters

In present study, we simply used basic interaction potential method to analyzed six SOECs and ten TOESs. For the zirconium metal, the crystal factors 'a' (basal plane factor) 'p' (axial proportion) as well as the value of density (ρ : $\times 10^3 \text{ kg m}^{-3}$), are 3.231 (Å) to 3.053 (Å), 1.514 to 1.621 as well as 19.357 to 21.948 under the given pressure interval 0-50 GPa, respectively [26]. Computed numeric values of thermal conductivity ($k_{(min)}$ Erg/cm.sec.K) is shown in figure 1, under the similar pressure interval. For zirconium metal, the established values of m as well as n stand 6 and 7. For the Zr metal, b_0 (chosen constant parameter) value is $1.88 \times 10^{-64} \text{ erg cm}^7$.

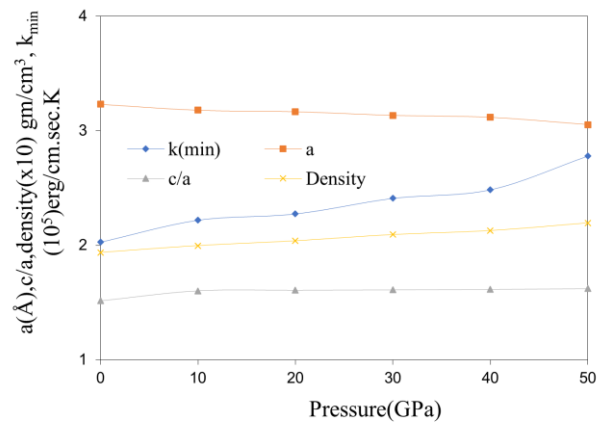


Fig. 1. Thermal conductivity, a (Å), c/a, density vs Pressure of Zr metal

The elastic coefficients values, which are significant for the material system since they are connected to the rigidity parameter, are located in the Zr metal. In fig. 2 (a) we can see that second order elastic constants (SOECs) are increasing with pressure. In fig. 2 (b) we can see that the value of third order elastic constants (TOECs) are negative and value of TOECs are increasing with pressure. The Ultrasonic attenuation (UA) and related properties are determined using SOECs. Zirconium metal has the sufficient elastic coefficients values indicating that it has higher mechanical characteristics than other compounds (Ti, Hf).

Consequently, the popular Born-Huang equilibrium law would be satisfied [27, 28] given by eqn. 18, for the hexagonal closed packed structure to being mechanically stable (fig. - 3)

$$\dot{C}_{44} > 0, \dot{C}_{11} - |\dot{C}_{12}| > 0, (\dot{C}_{11} + \dot{C}_{12}) \dot{C}_{33} - 2 \dot{C}_{13}^2 > 0, \quad (18)$$

Where $\dot{C}_{ij} = \dot{C}_{ij} - P$, (j=1, 3, 5). $\dot{C}_{12} = C_{12} + P$, $\dot{C}_{13} = C_{13} + P$

The fact that, the above mentioned elastic coefficients values are positive indicates that somehow this Zr metal satisfies Born- Huang's mechanical stability criterion, which implies that such stability grows within the specified pressure range. The evaluated value of bulk modulus of Zr metal is 99.40 GPa at zero pressure, which is close to 93.60 GPa calculated by Xiuxiu Yang et al.

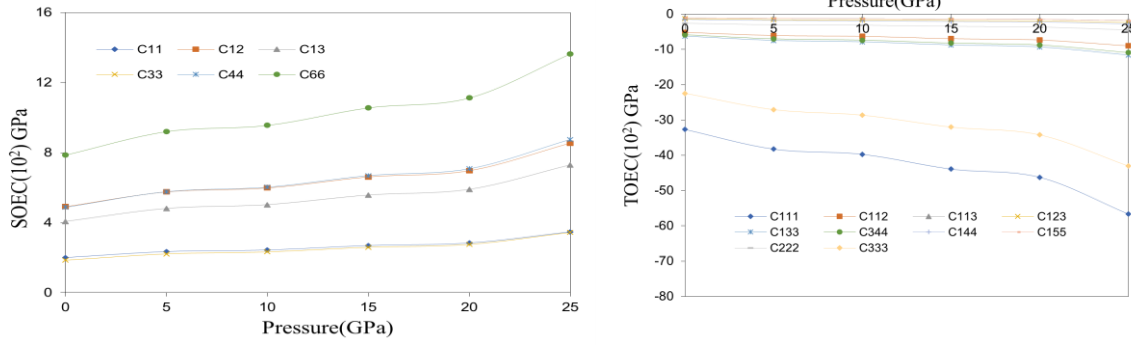


Fig. 2. SOECs and TOECs vs Pressure of Zr metal.

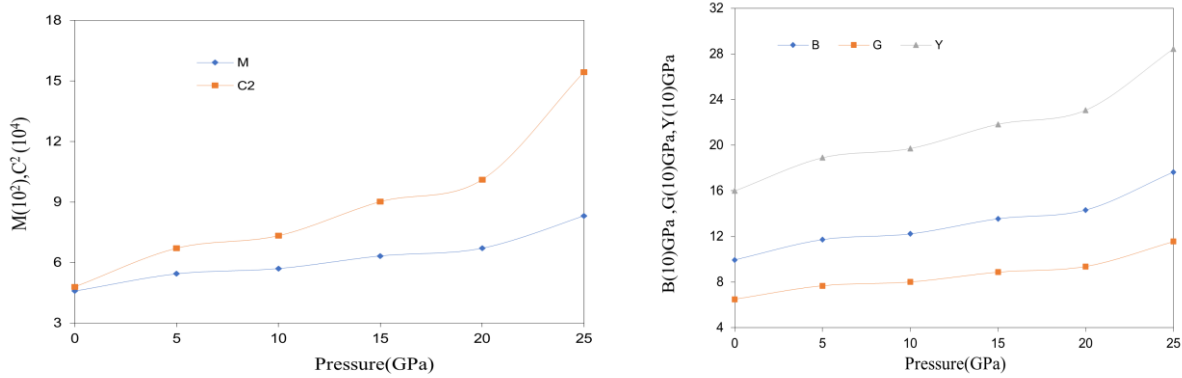


Fig. 3. M, C², B, Y, G versus Pressure of Zr metal.

[26]. Our approach achieves comparable magnitudes of the elastic constants C_{11} , C_{33} , and C_{66} . As a result, there is some consistency between reported and informed numeric values, which is due to elastic coefficients. Our theoretical strategy for assessing SOECs of hcp organized metals is therefore well supported.

The numeric values of Voigt–Reus’ coefficients (M as well as C^2), B , G , and Y as well as Poisson's proportion of Zr metal in the pressure range (0 to 25GPa) are calculated consuming Equation 9 are shown below in figs. 3 and 4.

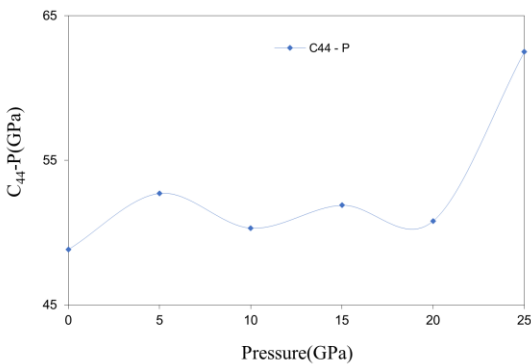


Fig. 4. C_{44} - P versus Pressure of Zr metal.

The SOECs allow for the evaluation of all mechanical characteristics, including toughness, brittleness, ductility, hardness, as well as compressibility. The melting point being taken into consideration when creating better materials. It is regarded as a crucial foundation for assessing engineering materials. Melting heats are being

studied by materials scientists in attempt to optimize the high thermal stability of any industrial applicable materials. In current work, the hardness and melting point temperature T_m of Zr metal is evaluated. Figure 5 illustrates the approximated melting point temperature as a consequence of the applied pressure. One can observe that as pressure rises, melting temperature rises as well as.

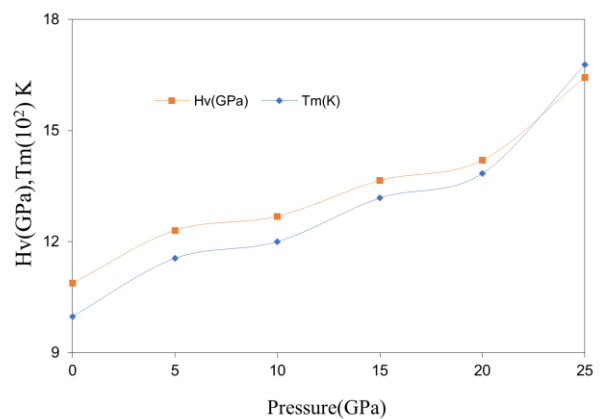


Fig. 5. Hardness (H_v), Melting point (T_m) with Pressure for Zr metal.

As illustrated in the table 1, anisotropy in elastic properties can be described by the universal anisotropic index (A^U), shear anisotropic factors (A_1 , A_2 as well as A_3), and percent anisotropy (A_B as well as A_G) and poisson ratio is provided below [29, 30]. By Table 1, its

Table 1.

Pressure dependent Anisotropy constants and Poission ratio (σ) of Zirconium Metal

Pressure (GPa)	A^U	A_B	A_G	A_1	A_2	A_3	σ
0	0.095	0.051	0.018	0.63	0.63	2.07	0.23
5	0.125	0.025	0.017	0.63	0.63	2.07	0.23
10	0.073	0.053	0.016	0.63	0.63	2.07	0.23
15	0.068	0.052	0.016	0.63	0.63	2.07	0.23
20	0.065	0.053	0.016	0.63	0.63	2.07	0.23
25	0.057	0.053	0.015	0.63	0.63	2.07	0.23

reveal that under different pressure points for Zr metal, percent anisotropy A_B is higher than A_G . This demonstrates that the orientation of the shear strength differs from the orientation of the bulk elastic modulus. Table 1 provides that A_1 , A_2 , and A_3 outcomes under various pressure. The metal is an isotropic crystal if $A_1 = A_2 = A_3 = 1$. It's an anisotropic material otherwise it is not an isotropic material, according to the conclusions. Strong single crystalline anisotropy is the term used to describe how far the universal anisotropy value (A^U) deviates from zero at different pressures [31, 32].

2.2. Thermal Relaxation Time, Velocities of Ultrasonic Waves and Related Parameters

Figure 6 depicts a graph of the estimated time required for thermal relaxing as a consequence of angle. The mutual relationship of V_D as $\tau \propto 3K/C_V V_D^2$ is observed by direction reliant curves. The duration of thermal repose of the Zr metal is clearly influenced by 'k', the duration of thermal relaxation is measured in picoseconds [33, 34]. The value of " for wave spread along = 55° indicates that the time to re-establish for thermal phonon distribution of equilibrium will be shortest for wave spread in this way due to phonon-phonon (p-p) interaction as well as relaxation due to heat, attenuation of ultrasonic waves occurs.

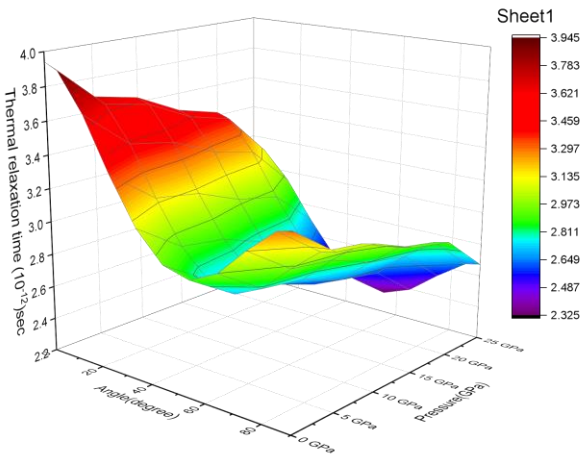


Fig. 6. Pressure dependent Relaxation time vs angle "Θ" of Zr metal.

Figures 7 to 8 depict the relationship between acoustic velocities and pressure. Figure 7(a), shows that for Zr metal value of V_L has the least value at 45° , as well as the numeric value of velocity V_{S1} has a supreme value at angle 55° in figure 7(b). Figure 8(a) shows that V_{S2} increases with angle along with the z- axis. The uneven

comportment of orientation reliant velocity is due to the existence of SOECs and solidity. The orientation based velocity curves reported in other hexagonal materials are analogous to the alliance based velocity curvatures seen in this investigation [30, 31]. The angle dependence of such velocities in the Zr metal combination is thus explained.

Figure 8(b) illustrates how the variation in Debye average velocity is influenced by the angle made with the crystal's unique axis. For the Zr metal, V_D rises with angle as well as reaches an extreme at 55° . Due to the fact that the velocities V_{S2} , V_{S1} and V_L are utilized in the calculation of V_D [33, 34]. At 55° , the extreme value of V_D is obtained by an important rise in both shear as well as longitudinal wave velocities, as well as a drop in quasi-shear wave velocities. When an acoustic wave propagate at 55° degree along with the z-axis of this crystal, the regular ultrasound wave velocity shows that the supreme. For zirconium metal, we estimated V_D , V_S as well as V_L .

In current work, the relationship between ultrasonic velocity and the isotropic and mechanical characteristics of the hcp organized metal is examined. Figure 9 shows the acoustic coupling coefficients (D_L as well as D_S) with pressure. The pressure-dependent C_V numeric values as well as the density of thermal energy (E_0) are determined consuming the physical coefficients are shown in Figure 10.

Figure 9 demonstrates that for Zr metal throughout all pressure, the numeric values of D_L are greater than D_S . It is evident that longitudinal ultrasound waves convert acoustical energy to heat energy more quickly than shear ultrasound waves.

2.3. Attenuation of Ultrasonic waves due to Phonon-Phonon Interaction

When calculating attenuation of ultrasonic waves (UA) in Zr metal, the wave is anticipated to move along the element's z-axis. The attenuation coefficient divides by the square of the frequency $(\alpha/f^2)_{Akh}$ is calculated for longitudinal acoustic wave $(\alpha/f^2)_L$ and for shear acoustic wave $(\alpha/f^2)_S$ using Eqn. 13, 14 and 15. Ultrasonic attenuation caused due to phonon- phonon interaction for zirconium metal is shown in figure 11 given below.

In this current work, it is anticipated that the acoustic wave will move along the z-axis of the crystal. It is obvious that the Akh. Type of energy waste $(\alpha/f^2)_{Akh}$ depends on the D , E_0 , τ and V^{-3} (Eqns. 15). E_0 as well as the k significantly affect Akhiezer losses in zirconium metal.

Therefore, a diminution in the capacity to transfer heat is the cause of the increase in Acoustic attenuation. As a result, the phonon-phonon interaction influences acoustic

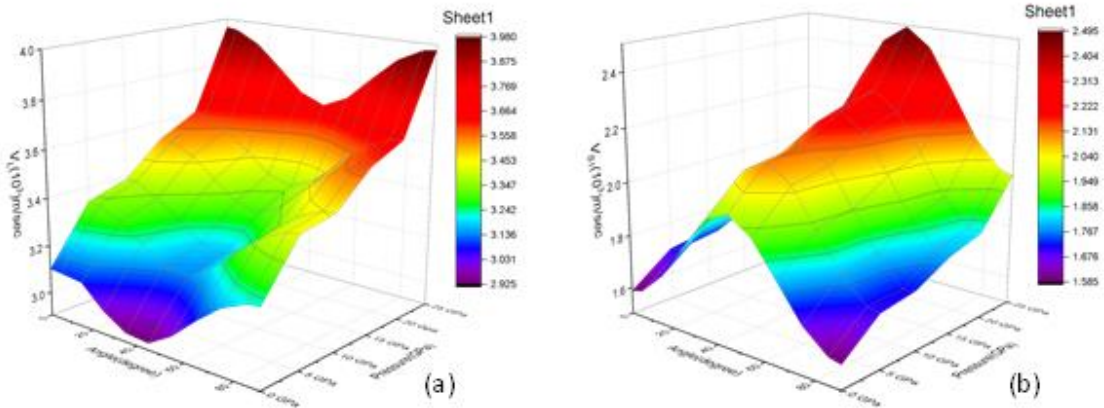


Fig. 7. Pressure dependent V_L, V_{S1} vs angle " θ " of Zr metal.

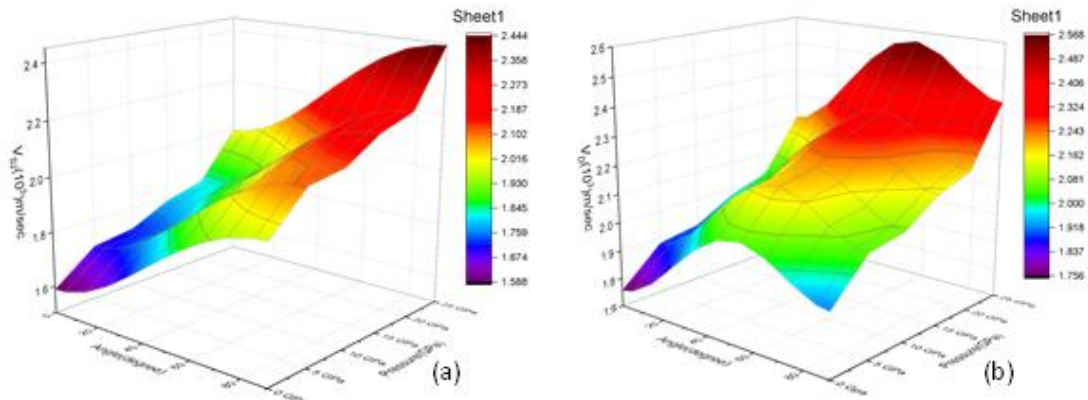


Fig. 8. Pressure dependent V_{S2}, V_D vs angle " θ " of Zr metal

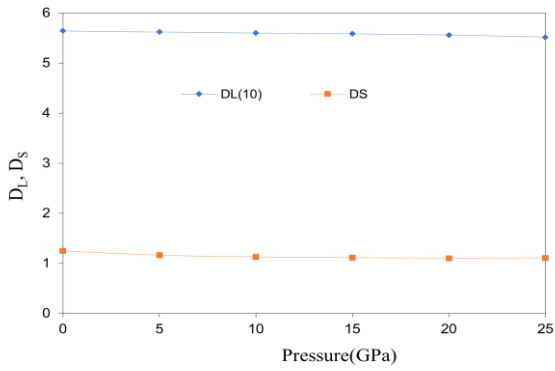


Fig. 9. D_L, D_S vs Pressure of Zr metal

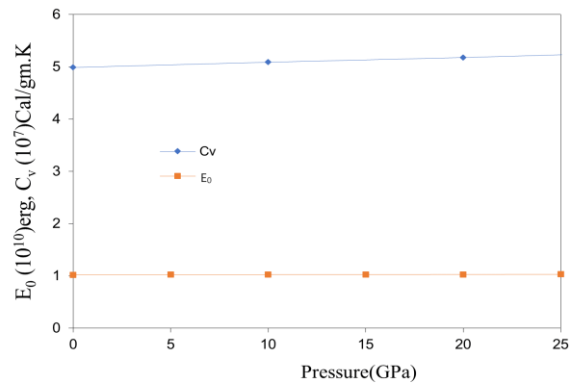


Fig. 10. E_0, C_v for Zr metal with pressure

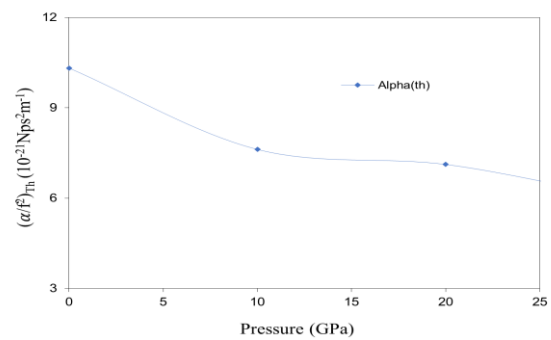
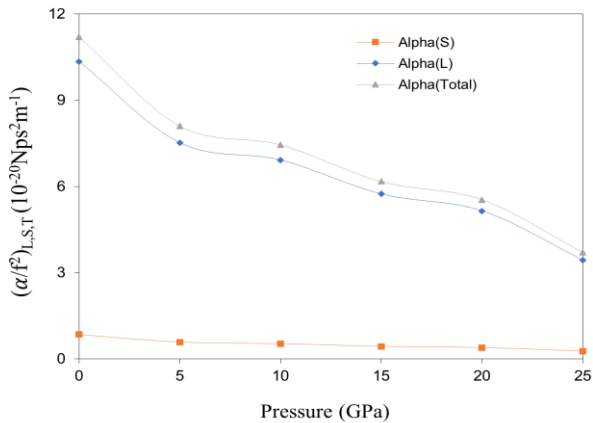


Fig. 11. Long., Shear & Th. attenuation vs Pressure of Zr metal.

attenuation, however, due to an absence of hypothetical/investigational evidence in the collected works, a contrast of attenuation of ultrasonic waves (UA) is not possible. Both the overall attenuation employing Eqn. 17 and Eqn. 16 demonstrate that now the thermo-elastic degeneration for Zirconium metal is significantly less than Akhiezer loss. The main contributing factor is acoustical attenuation due to p-p interactions for longitudinal acoustic wave as well as shear wave. Thermal conductivity and thermal energy density are the two main determinants of total acoustical attenuation. The Zirconium metal maintains its hcp structural configuration, which is highly stable, at low values of acoustic wave's attenuation under various pressures.

Conclusions

In current theoretical approach, the interaction potential technique is used to evaluate the mechanical as well as thermodynamic properties of the Zr metal under pressures ranging from 0 to 25 GPa. At various pressures, the idea of calculating higher-order elastic coefficients for hcp shaped Zr metal using an easy interaction potential methodology is still relevant. Born-Huang mechanical stability standard demonstrates that, within the operating pressure, Zr metal's mechanical stability increases with pressure. According to the Paugh ratio, the hexagonal Zirconium metal is bendable under both normal

and the given pressure range, and its ductility rises as pressure rises. Additionally, we discovered that Zr metal exhibits strong anisotropy at zero GPa, which intensifies with increasing pressure. With increasing pressure, the Debye average velocity rises and then decreases. Pressure raises the estimated melting point and toughness of Zr metal.

The hardness (H_v) increases smoothly with increasing pressure until it exceeds 0-25 GPa. ' τ ' is shown to be of the order of picoseconds for Zr metal, protecting their hexagonal shape. Because ' τ ' has the least value alongside = 55° at altogether pressures, the time essential for re-establishing phonon evenness spreading will be the tiny for acoustical wave transmission in this direction. The primary factor in overall attenuation caused by the p-p strong interaction is thermal conductivity. At the stated pressure range, Zr metal are in their original physical state and are more malleable, as seen by the least ultrasonic attenuation (UA). The findings could aid in the processing of Zr metal and non-destructive characterization. Future exploration interested in the thermo-physical characteristics of other substances will be based on these conclusions.

Prashant Srivastav – Ph.D. Research Scholar;
Aadesh K. Prajapati – Ph.D. Assistant Professor;
Pramod K. Yadawa – Ph.D., Professor & Director.

- [1] J.C. Jamieson, *Crystal Structures of Titanium, Zirconium, and Hafnium at High Pressures*, Science 140, 72 (1963); <https://doi.org/10.1126/science.140.3562.72>.
- [2] A. Jayaraman, W. Klement, G.C. Kennedy, *Solid-Solid Transitions in Titanium and Zirconium at High Pressures*, Phys. Rev. 131, 644 (1963); <https://doi.org/10.1103/PhysRev.131.644>.
- [3] M.P. Usikov, V. Zilbersh, *The orientation relationship between the α - and ω -phases of titanium and zirconium*, Phys. Status Solidi A 19, 53 (1973); <https://doi.org/10.1002/pssa.2210190103>.
- [4] A. Rabinkin, M. Talianker, O. Botstein, *Crystallography and a model of the $\alpha \rightarrow \omega$ phase transformation in zirconium*, Acta Metall. Mater 29, 691 (1981); [https://doi.org/10.1016/0001-6160\(81\)90152-8](https://doi.org/10.1016/0001-6160(81)90152-8).
- [5] B. Stauder, C. Frantz, *Mise en evidence d'une phase omega dans des films minces de zirconium et zirconium-oxygene realises par pulverisation cathodique magnetron*, Scripta Metall. Mater 25, 2127 (1991); [https://doi.org/10.1016/0956-716X\(91\)90286-A](https://doi.org/10.1016/0956-716X(91)90286-A).
- [6] A.V. Dobromyslov, N.V. Kazantseva, *Formation of metastable ω -phase in Zr-Fe, Zr-Co, Zr-Ni, and Zr-Cu alloys*, Scripta Materialia 37, 615 (1997); [https://doi.org/10.1016/S1359-6462\(97\)00168-1](https://doi.org/10.1016/S1359-6462(97)00168-1).
- [7] Y.K. Vohra, *Kinetics of phase transformations in Ti, Zr and Hf under static and dynamic pressures*, Journal of Nuclear Materials 75, 288 (1978); [https://doi.org/10.1016/0022-3115\(78\)90010-7](https://doi.org/10.1016/0022-3115(78)90010-7).
- [8] S.A. Catledge, P.T. Spencer, Y. K. Vohra, *Nanoindentation hardness and atomic force microscope imaging studies of pressure-quenched zirconium metal*, Applied Physics Letters 77, 3568 (2000); <https://doi.org/10.1063/1.1329632>.
- [9] Y. Zhao, J. Zhang, *Enhancement of yield strength in zirconium metal through high-pressure induced structural phase transition*, Applied Physics Letters 91, 201907 (2007); <https://doi.org/10.1063/1.2802726>.
- [10] R. Ahuja, L. Dubrovinsky, N. Dubrovinskaia, J. M. Osorio, M. Mattesini, B. Johansson, T. Le Bihan, *Titanium metal at high pressure: Synchrotron experiments and ab initio calculations*, Phys. Rev. B 69, 184102 (2004); <https://doi.org/10.1103/PhysRevB.69.184102>.
- [11] E. Cerrera, G. T. Gray, R. S. Hixson, P. A. Rigg, D. W. Brown, *The influence of interstitial oxygen and peak pressure on the shock loading behavior of zirconium*, Acta Materialia 53, 1751 (2005); <https://doi.org/10.1016/j.actamat.2004.12.024>.
- [12] G. Jyoti, S.C. Gupta, *Theoretical analysis of the isostructural transition in Zr at 53 GPa*, Journal of Physics: Condensed Matter 6, 10273 (1994); <https://doi.org/10.1088/0953-8984/6/47/010>.
- [13] D.K. Pandey, P.K. Yadawa, R.R. Yadav, *Ultrasonic properties of hexagonal ZnS at nanoscale*, Mater. Lett. 61, 5194 (2007); <https://doi.org/10.1016/j.matlet.2007.04.028>.

- [14] P.K. Yadawa, *Computational Study of Ultrasonic Parameters of Hexagonal Close-Packed Transition Metals Fe, Co, and Ni*, Arabian Journal for Science and Engineering 37, 255 (2012); <https://doi.org/10.1007/s13369-011-0153-6>.
- [15] A. K. Prajapati, S. Rai, Kuldeep, P.K. Yadawa, *Pressure dependent elastic, mechanical and ultrasonic properties of ZnO nanotube*, Indian Journal of Pure & Applied Physics 61, 115 (2023); <https://doi.org/10.56042/ijpap.v61i2.64116>.
- [16] V. Rajendran, A. Marikani, Material Science, Tata McGraw Hill Publisher, 2, 29(2009).
- [17] S.O. Pillai, Solid State Physics: Crystal Physics (New Age International Publisher, London, 2005).
- [18] A.K. Prajapati, S. Rai, P.K. Yadawa, *Pressure-Dependent Elastic, Mechanical, Thermo-Physical and Ultrasonic Properties of Titanium Diboride*, MAPAN- JMSI 37, 597 (2022); <https://doi.org/10.1007/s12647-022-00590-1>.
- [19] D. Singh, D.K. Panday, P.K. Yadawa, A.K. Yadav, *Attenuation of ultrasonic waves in V, Nb and Ta at low temperatures*, Cryogen 49, 12 (2009); <https://doi.org/10.1016/j.cryogenics.2008.08.008>.
- [20] P.K. Yadawa, D. Singh, D.K. Panday, R.R. Yadav, *Elastic and Acoustic Properties of Heavy Rare-Earth Metals*, The Open Acoustics Journal 2, 61 (2009); <http://doi.org/10.2174/1874837600902010061>.
- [21] R. Hill, *The Elastic Behaviour of a Crystalline Aggregate*, Proc. Phys. Soc. A 65, 349 (1952); <http://doi.org/10.1088/0370-1298/65/5/307>.
- [22] N. Turkdal, E. Deligoz, H. Ozisik and H.B. Ozisik, *First-principles studies of the structural, elastic, and lattice dynamical properties of ZrMo₂ and HfMo₂*, Ph. Transit. 90, 598 (2017); <https://doi.org/10.1080/01411594.2016.1252979>.
- [23] P.F. Weck, E. Kim, V. Tikare, J.A. Mitchell, *Mechanical properties of zirconium alloys and zirconium hydrides predicted from density functional perturbation theory*, Dalton Trans. 44, 18769 (2015); <https://doi.org/10.1039/C5DT03403E>.
- [24] T. Morelli Donald and A. Slack Glen, High lattice thermal conductivity solids in high thermal conductivity of materials in S. L. Shinde (Springer Publisher, 2006).
- [25] M.E. Fine, L.D. Brown, H.L. Marcus, *Elastic constants versus melting temperature in metals*, Scripta Metallurgica 18, 951 (1984); [https://doi.org/10.1016/0036-9748\(84\)90267-9](https://doi.org/10.1016/0036-9748(84)90267-9).
- [26] X. Yang, S. Zhang, H. Zhu, P. Tao, L. Huang, M. Li, W. Zhang, Y. Li, C. Zhou, and Y. Zou, *Structural Stability, Thermodynamic and Elastic Properties of Cubic Zr_{0.5}Nb_{0.5} Alloy under High Pressure and High Temperature*, Crystals 12, 631 (2022); <https://doi.org/10.3390/cryst12050631>.
- [27] S. Rai, N. Chaurasiya, P.K. Yadawa, *Elastic, Mechanical and Thermophysical properties of Single-Phase Quaternary ScTiZrHf High-Entropy Alloy*, Physics and Chemistry of Solid State 22, 687 (2021); <http://doi.org/10.15330/pcss.22.4.687-696>.
- [28] X.K. Liu, W. Zhou, X. Liu, S.M. Peng, *First-principles investigation of the structural and elastic properties of Be₁₂Ti under high pressure*, RSC Adv. 5, 59654 (2015); <https://doi.org/10.1039/C5RA11249D>.
- [29] A.L. Ivanovskii, *Hardness of hexagonal AlB₂-like diborides of s, p and d metals from semi-empirical estimations*, Int. J. Refract. Met. Hard Mater 36, 183 (2013); <https://doi.org/10.1016/j.ijrmhm.2012.08.013>.
- [30] A. Guechi, A. Merabet, M. Chegaar, A. Bouhemadou, N. Guechi, *Pressure effect on the structural, elastic, electronic and optical properties of the Zintl phase KAsSn, first principles study*, J. Alloys Compd. 623, 219 (2015); <https://doi.org/10.1016/j.jallcom.2014.10.114>.
- [31] S.I. Ranganathan, M. Ostoja-Starzewski, *Universal Elastic Anisotropy Index*, Phys. Rev. Lett. 101, 9007 (2008); <https://doi.org/10.1103/PhysRevLett.101.055504>.
- [32] K.B. Panda, K.S. Ravi Chandran, *Determination of elastic constants of titanium diboride (TiB₂) from first principles using FLAPW implementation of the density functional theory*, Comput. Mater. Sci. 35, 134 (2006); <https://doi.org/10.1103/PhysRevLett.101.055504>.
- [33] S.P. Singh, G. Singh, A.K. Verma, P.K. Yadawa, R.R. Yadav, *Ultrasonic wave propagation in thermoelectric ZrX₂(X=S,Se) compounds*, Pramana-J. Phys. 93, 83 (2019); <https://doi.org/10.1007/s12043-019-1846-8>.
- [34] A.K. Jaiswal, P.K. Yadawa, R.R. Yadav, *Ultrasonic wave propagation in ternary intermetallic CeCuGe compound*, Ultrasonics 89, 22 (2018); <https://doi.org/10.1016/j.ultras.2018.04.009>.

П. Шривастав, А.К.Праджапаті, П.К.Ядава

Теоретичні дослідження термічних, механічних та ультразвукових властивостей металевого цирконію під тиском

Кафедра фізики, В. Б. С. Університет Пурванчал, Джаунпур, Індія, pkvadawa@gmail.com

Цирконій (Zr), метал hcp структури, досліджено передачею акустичних хвиль при робочому тиску від 0 до 25 ГПа. Для цього використано підхід потенціалу взаємодії Леннарда-Джонса для оцінки коефіцієнтів пружності вищого порядку (SOEC і TOEC). Ця модель використовується для розрахунку пружних параметрів 2-й та 3-й порядки для металевого цирконію. За допомогою SOEC були розраховані інші модулі пружності, такі як об'ємний модуль (B), модуль Юнга (Y) і модуль зсуву (G) для Zr із використанням наближень Фойгта-Ройсса-Хілла (VRH). Потім, застосовуючи SOECs, а також щільність цирконію в тому самому діапазоні тиску, було вивчено три залежні від орієнтації швидкості звуку, що містять середні швидкості Дебая. Основні теплові характеристики, такі як питома теплоємність при постійному об'ємі, ґраткова теплопровідність, густина теплової енергії, час теплової релаксації, а також коефіцієнти акустичного зв'язку металевого цирконію розраховано в тих самих ж діапазонах тиску. Розрахунок є задовільним для оцінки коефіцієнтів ослаблення ультразвуку, що виникає внаслідок взаємодії фононів, твердості, а також температури плавлення під різними тисками.

Ключові слова: ультразвукові властивості, пружні константи, термо-фізичні характеристики, теплопровідність.